Journal of Chemical and Petroleum Engineering (JChPE)

Print ISSN: 2423-673X Online ISSN: 2423-6721

Liner Pressure Test Buckling Generation and Influences on Running String and Cement Quality of Previous Casing in Vertical Wells

Leksir Abdeslem *

Department of Engineering, Drilling Direction, SONATRACH, Hassi Messaoud, Algeria. E-mail: leksir1@yahoo.fr

ARTICLE INFO

Article History:
Received: 23 March 2022
Revised: 08 March 2023
Accepted: 11 March 2023

Article type: Research

Keywords:
Buckling Generation,
Casing Pressure Test,
Gaze Migration,
Running String Buckling,
Well Integrity

ABSTRACT

Buckling occurrence during liner pressure test represents a challenge, in addition to running string deformation; previous casing cement quality may be severely affected. Practically, the running string is placed straightly on the top of the liner. Consequently, the buckling pressure limit will surely be reached while rising pressure. In order to investigate column performances during testing, drill pipe elongation, bending, and buckling are all considered. Buckling influences on pipe quality, based on helical springs under compression theory will be revisited. The examination of contact pressure generated and their influences on previous casing cement sheath is the main purpose, via interface continuity conditions and stress analysis method. Results show that minimum yield shear stress could be achieved at high casing pressure tests. Conversely, contact pressure, radial and hoop stress, for both interfaces casing-cement and cement-formation confirm that DP has more influences on cement sheath compared to the casing. Simulations and well registrations were presented to confirm buckling occurrence and their impacts.

Introduction

The liner is a column that does not extend to the surface but hangs inside the previous casing. Techniques of running, cementing, and testing represent the key success of the sealing mechanism [1-3]. Several phenomena could take place during operation execution, such as Euler elongation [4], buckling, ballooning, piston effect, and temperature variations [5]. Different from the casing, buckling during the liner pressure test will influence running string only (Drill pipe, DP). This later makes buckling generation inevitable, since the running tool is initially buckled by slack-off weight [6]. As Compressive force initiates, a neutral point rises inside the column [7], and bending and buckling take place and affect drill pipe quality and/or cement behind the casing [8].

Neutral point position receives huge variations due to fluid characteristics change during slurry pumping and displacement [7, 9]. A new method to analyze buckling in inclined wells referred to as "Paslay force" was presented by Chen [10] and Mitchell [11]. Other studies emphasize completion systems [12-14] or horizontal wells [15-20]. In vertical sections, buckling occurs at relatively low compressive force compared to horizontal ones [21]. Liner running string (DP) is located in the previous casing interval; hence, any buckling may affect the cement behind.

* Corresponding Author: L. Abdeslem (E-mail address: leksir1@yahoo.fr)

Journal of Chemical and Petroleum Engineering, 2023, 57(1): 149- 165.
Publisher: University of Tehran, College of Engineering DOI: 10.22059/jchpe.2023.340239.1385

In order to study buckling influences on drill pipe characteristics, helical spring under compression [22] and Hertzian cylindrical contact theories [23], were used to investigate and select drill pipe usability interval. Stress evolution while column testing is exanimated, then a comparison between casing and liner testing is presented. The severity factor used to evaluate the magnitude of stress is the evolution from homogeneous mud to the new complex cementing system; conjointly with the gap between casing and liner buckling conditions.

The liner will have special behavior while testing [21], surface pressure pushes inside hydrostatic to overcome the outside one. Buoyancy force receives huge variations, and additional compressive force generated leads to DP elongation [24]. More specifications concerning buoyancy changes are presented in [25, 26]. Knowing that the drill pipe was initially slacked-off on top of the liner, increasing inside pressure will produce extra compressive force [27].

Liner Column Pressure Testing and Buckling Generation

The cement job is the operation which guarantees the efficiency of the sealing system [28, 29], via mud removal and slurry placement [30, 31], cement sheath preserves the integrity of the well. At the end of each cementing operation, a pressure test must run, to confirm the reliability of the mechanism [32].

DP stretches longitudinally while testing, setting tool sealed-off the flow itinerary without supporting the entire weight. Space out between the setting tool and the top liner is practically valueless, hence any elongation will convert to helical buckling. As pressure raises the number of helix pitches increases. Each new pitch created needs more compressive force and exerts an additional force on the previous casing's inner wall. As compressive force rises, contact pressure generated and exerted by DP increases. Assured by interface continuity conditions theory, similar stress applied toward the internal interface (casing-cement interface) may affect the integrity of cement [33].

Fig. 1 below gives an overview of buckling generation during the casing and liner pressure test. The liner is off-bottom and their elongation will not reach TD, compared to the consolidated casing column where buckling initiation is conditioned by touching TD. Accordingly, DP buckling will affect the previous casing and cement behind. Consequences vary from simple bending, tubular permanent deformation, and total shear of the string to breakout cement sheath behind.

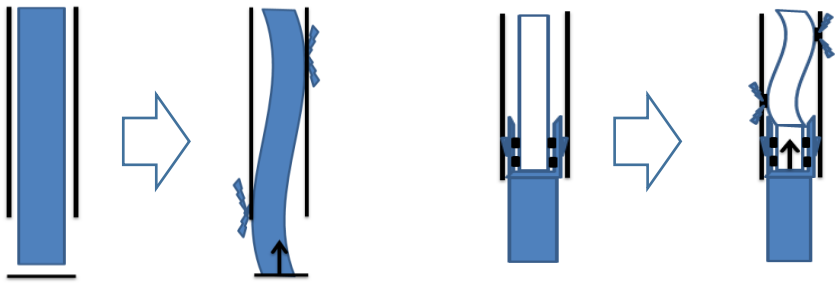

(a) Casing buckling (b) Drill pipe buckling (Liner)

Fig. 1. Drill pipe/Casing buckling during final pressure test

Model of DP Buckling while Pressure Testing of Liner in Vertical Wells

Suspended string exposed to tension force generated by column weight, fluid density, and flow rate variations will influence the total weight suspended via changing buoyancy force [34].

Casing Buckling force is given by [9], as follows:

$$F_b = F_a + A_i P_i - A_o P_o \quad (1)$$

F_b: Buckling force, (lbf). F_a: DP tension force. (lbf). Additional variable force ($A_i P_i - A_o P_o$) related to downhole conditions. Where A_i: Area of DP internal diameter (in^2). A_o: Area of DP outer diameter (in^2). P_i: Equivalent inside bottom pressure (psi). P_o: Equivalent annulus bottom pressure (psi).

Leksir in [34] presents a point of view to define buckling during cementing. Displacing slurry inside the casing, may lead to overcoming outside equivalent behavior $A_o P_o$ by inside $A_i P_i$ one. More precisely, the additional force generated ($A_i P_i - A_o P_o$) remarkably lower compared to conventional homogenous systems ($A_i - A_o) P_h$. Consequently, more column weight was recovered and additional elongation was produced. The same risk may occur during the final liner pressure test, even if the outside equivalent hydrostatic pressure is slightly higher than the inside one, high pressure may cause elongation of DP.

Via the utilization of tubular elongation theory [4], the same considerations will apply to drill pipe during liner column testing. The equation of string elongation given by Leksir [34]:

$$E = (Fa - (AoPo - AiPi) * (L)/(735294 * w) \quad (2)$$

w is the buoyed weight per unit length (lbf/in), W is defined by [9] as: $W = W_s + W_i - W_o$. W_s is the weight of steel per unit length (lbf/in), W_i is the weight of fluid inside the casing per unit length (lbf/in), W_o is the weight of fluid outside the casing per unit length (lbf/in).

As elongation start, buckling takes place, and compressive force $\boldsymbol{F_{cr}}$ initiate. The buckling equation will be:

$$F_{bN} = F_b - F_{cr} \quad (3)$$

where F_{bN} is new buckling force and F_b is buckling force. The contact force F_N acted toward wellbore given by [13]:

$$F_N = (F_{cr}^2 r)/(4EI) \quad (4)$$

Before testing, compressive force $F_{cr} = 0$ and contact force is valueless. When the liner column elongates, $F_{cr} \neq 0$ and $F_N \neq 0$. As compressive force increases, straight columns convert to helically shaped structure; helix pitch P_{Pitch} calculated as follows [9]:

$$P_{Pitch} = \sqrt{8\pi^2 EI/F_{cr}} \quad (5)$$

In Eq. 5 when compressive force increases the helix pitch value decrease. This means the number of helix circles rises and the column tends to compact. Keep increasing pressure leads to generating a more compressive force.

The maximum contact pressure at the tubular interaction axe is given by the relation below [23]:

$$P_{max} = \frac{2 * F_{contact}}{\pi a} = \frac{F_{contact} * E_e}{\pi R_e} \quad (6)$$

where: $\frac{1}{E_e} = 2\frac{1-\nu^2}{E}$; $\frac{1}{R_e} = \frac{1}{R_2} - \frac{1}{R_1}$; E, ν are the young modulus and poisons ratio of the tubular; R_1, R_2 are the radius of DP and casing respectively, and a represents the contact area between DP and casing.

Maximum contact pressure exerted by DP transferred to the inner side of the cement throughout the casing. In this work only inside casing, casing-cement, and cement-formation stresses are investigated. Continuity conditions require the stress at interfaces steel, casing, and cement in initial and buckling situations to satisfy:

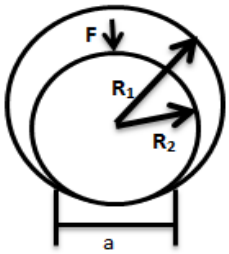

Initial situation:

$$\begin{aligned} \sigma_{R:in-CSG} &= -P_i \\ \sigma_{R:in-Cem} &= \sigma_{R:out-CSG} \\ \sigma_{R:out-Cem} &= \sigma_{R:in-For} \end{aligned} \tag{7}$$

Inside stress ($\sigma_{R:in-CSG}$) determined simply by hydrostatic pressure generated by fluids. Stress exerted on cement ($\sigma_{R:out-Cem}$) is equivalent to the stress applied by formation on cement.

Buckling situation:

$$\begin{aligned} \sigma_{R:in-CSG} &= -P_i - P_{max} \\ \sigma_{R:in-Cem} &= \sigma_{R:out-CSG} \\ \sigma_{R:out-Cem} &= \sigma_{R:in-For} \end{aligned} \tag{8}$$

At the contact axe, maximum pressure resulting from buckling is acting conjointly with initial stress. Assuming that the system is in an equilibrium state primarily, formation stress applied on cement is equivalent to inside hydrostatic pressure. The cement sheath-cracking limit is calculated by comparing maximum contact pressure to cement compressive strength. If the value of P_{max} exceed the strength limit of cement, cracking is expected to occur.

Assuming that P_{max} reached the cracking limit of cement behind the casing P_{crack}. The maximum surface pressure that could achieve before cracking the cement matrix is presented in the relation below:

$$P_{max} = \frac{\sqrt{\frac{4P_{crack}\pi EIR_e}{rE_e}} - A_o(P_h - P_o)}{A_i} \tag{9}$$

If the helix pitch number increases, pushed by excessive axial compressive load, to reach the limit where shear stress loading of DP is equal to minimum yield shear stress. The critical force required to raise the maximum shear to reach the minimum yield shear given in Eq. 10 below [35]:

$$F_{critic} = \pi d^2 t/4[(2D/d) + 1] \tag{10}$$

where F_{critic} (lbs) is the critical force required to raise the maximum shear to reach the minimum yield shear of DP, d (in) is the DP diameter, D (in) is the previous casing inside diameter, and t (psi) is half of the tensile yield.

Maximum surface pressure is reached, before axial compressive load reaches the limit where shear stress loading is equal to minimum DP yield shear stress, defined by the relation below:

$$F_{critic} = \pi d^2 t/4[(2D/d) + 1] \quad (11)$$

$$F_{cr} = A_i P_i - A_o P_o + (A_o - A_i) P_h \quad (12)$$

Knowing that while testing $P_i = P_h + P_{crit}$, the new relation of compressive load given by:

$$F_{cr} = A_i P_h + A_i P_{crit} - A_o P_o + (A_o - A_i) P_h = F_{critic} \quad (13)$$

$$P_{max} = \frac{F_{critic} - A_o(P_h - P_o)}{A_i} \quad (14)$$

Practically, even if minimum yield shear stress is not achieved, the plastic stage could easily attain.

Stress Analysis of Liner Helical Buckling String in Vertical Wells

In the composite cylinder under consideration, internal pressure Pi acting on the inner side of the previous casing conjointly with buckling contact pressure, cement sheath will resist expansion.

Considering casing–the cement interface, *Pi* is the internal pressure, Pc the contact pressure engenders by buckling; and Pc1 the contact pressure formed at cement–casing interface.

Assuming that the contact force distributed between the drill pipe and the previous casing is uniform, and neglecting the thermal expansion.

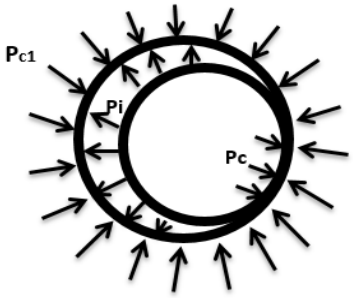

The hoop and axial strain given by [36]:

$$\varepsilon_\theta = \frac{1}{E}[\sigma_\theta - \boldsymbol{\nu}(\sigma_z + \sigma_r)] \quad (15)$$

$$\varepsilon_z = \frac{1}{E}[\sigma_z - \boldsymbol{\nu}(\sigma_\theta + \sigma_r)] \quad (16)$$

Founded on the large gap between casing depth and axial strain, this was later treated as valueless$\varepsilon_z \approx 0$. The axial stress will be:

$$\sigma_z = \boldsymbol{\nu}(\sigma_\theta + \sigma_r) \quad (17)$$

Since the axial strain is negligible considering the large depth, then (i.e. plane strain assumption). It follows from Eq. 15 that:

$$\varepsilon_\theta = \frac{1}{E}[\sigma_\theta(1 - \boldsymbol{\nu^2}) - \sigma_r(\boldsymbol{\nu} + \boldsymbol{\nu^2})] \quad (18)$$

The general expression of the radial expansion is given by:

$$\delta_r = \frac{r}{E}[\sigma_\theta(1-\boldsymbol{\nu^2}) - \sigma_r(\boldsymbol{\nu}+\boldsymbol{\nu^2})] \tag{19}$$

Considering the casing as a thin-walled vessel we have an outer diameter $r = R_2$, $\delta_r = -P$ and $\sigma_\theta = \frac{Pr_m}{t_s}$, where $P = (P_{test} + P_c) - P_{c1}$; $r_m$is the mean radius of the casing and t_s is the thickness of the casing.

The new presentation of the radial expansion δ_r given as follow:

$$\begin{aligned} \delta_r &= \left[\frac{R_2((P_i+P_c)-P_{c1})}{E}[\frac{r_m}{t_s}(1-\boldsymbol{\nu^2}) + (\boldsymbol{\nu}+\boldsymbol{\nu^2})\right] \\ (P_i+P_c) - P_{c1} &= \left[\frac{E}{R_2}(\delta_r)\frac{1}{\frac{r_m}{t_s}(1-\boldsymbol{\nu^2}) + (\boldsymbol{\nu}+\boldsymbol{\nu^2})}\right] \end{aligned} \tag{20}$$

The final formula of P_{c1} with buckling contact pressure included given by:

$$P_{c1} = (P_i+P_c) - \left[\frac{E}{R_2}(\delta_r')\frac{1}{\frac{r_m}{t_s}(1-\boldsymbol{\nu^2}) + (\boldsymbol{\nu}+\boldsymbol{\nu^2})}\right] \tag{21}$$

At the initial conditions without buckling, P_{c1}will be:

$$P_{c1} = P_i - \left[\frac{E}{R_2}(\delta_r)\frac{1}{\frac{r_m}{t_s}(1-\boldsymbol{\nu^2}) + (\boldsymbol{\nu}+\boldsymbol{\nu^2})}\right] \tag{22}$$

The variation of radial stress will be:

$$(\delta_r' - \delta_r) = \frac{R_2 P_c}{E}[\frac{r_m}{t_s}(1-\boldsymbol{\nu^2}) + (\boldsymbol{\nu}+\boldsymbol{\nu^2})] \tag{23}$$

Contact pressure P_{c1} and P_{c2} are correlated by the relation below [36]:

$$A\,P_{c1} + B\,P_{c2} = C \tag{24}$$

where:

$$A = \left[\frac{b}{E_c}\left[(1-\boldsymbol{\nu_c^2})\left[\frac{b^2+c^2}{c^2-b^2}\right] + (\boldsymbol{\nu_c}+\boldsymbol{\nu_c^2})\right] + \frac{a}{E_s}\left[\frac{\boldsymbol{r_m}}{\boldsymbol{t_s}}(1-\boldsymbol{\nu_s^2}) + (\boldsymbol{\nu_s}+\boldsymbol{\nu_s^2})\right]\right]$$

$$B = \frac{b}{E_c}\left[(1-\boldsymbol{\nu_c^2})\left[\frac{2c^2}{c^2-b^2}\right]\right]$$

$$C = \frac{p_i a}{E_s}\left[\frac{\boldsymbol{r_m}}{\boldsymbol{t_s}}(1-\boldsymbol{\nu_s^2}) + (\boldsymbol{\nu_s}+\boldsymbol{\nu_s^2})\right]$$

Knowing that the contact pressure $P_{c2}$to the formation, equals to the confining pressure and there is no restriction in the movement of cement sheath by the formation. P_{c1} given by:

$$P_{c1} = \frac{C - B\,P_{c2}}{A} \tag{25}$$

As contact pressuresP_{c1}, P_{c2} known, stress matrix applied on casing and cement could easily be calculated.

Circumferential stress

$$\sigma_\theta(r) = P_{c1}\frac{b^2}{c^2 - b^2}\frac{1 + c^2}{r^2} - P_{c2}\frac{c^2}{c^2 - b^2}\frac{1 + b^2}{r^2} \tag{26}$$

Radial stress

$$\sigma_r(r) = P_{c1}\frac{b^2}{c^2 - b^2}\left(1 - \frac{c^2}{r^2}\right) - P_{c2}\frac{c^2}{c^2 - b^2}\left(1 - \frac{b^2}{r^2}\right) \tag{27}$$

During buckling $P = (P_i + P_c - P_{c1})$; $r = b$

$\sigma_r = -P$ and $\sigma_\theta = \frac{Pr_m}{t_s}$

$\sigma_r' = -(P_i + P_c - P_{c1})$ and $\sigma_\theta' = \frac{(P_i + P_c - P_{c1})r_m}{t_s}$

$P_{c1} = -(P_i + P_c) + \sigma_r'$ and $P_{c1} = P_i + P_c - \frac{t_s}{r_m}\sigma_\theta'$

During testing $P_{c1} = (P_i - P_{c1})$

$\sigma_r = -P$ and $\sigma_\theta = \frac{Pr_m}{t_s}$

$\sigma_r = -(P_i - P_{c1})$ and $\sigma_\theta = \frac{(P_i - P_{c1})r_m}{t_s}$

$P_{c1} = \sigma_r - P_i$ and $P_{c1} = -\frac{t_s}{r_m}\sigma_\theta + P_i$

Radial and tangential stress evolution while buckling is given below:

$\sigma_r' - \sigma_r = P_c$ and $\sigma_\theta' - \sigma_\theta = P_c\frac{r_m}{t_s}$

Projection of Radial and tangential stress evolution at r = b is substituted into Eq. 27, this gives the radial expansion in the cement sheath as

$$\delta_r = \frac{b}{E_c}\left[(1 - \boldsymbol{\nu^2})\left[P_{c1}\left(\frac{b^2 + c^2}{c^2 - b^2}\right) - P_{c2}\left(\frac{2c^2}{c^2 - b^2}\right)\right] + P_{c1}(\boldsymbol{\nu} + \boldsymbol{\nu^2})\right] \tag{28}$$

Following the same strategy used for casing, cement interface expansion evolution during buckling is given by:

$$\delta_r = \frac{b}{E_c}\left[(1 - \boldsymbol{\nu^2})\left[(P_{c1} + P_i + P_c)\left(\frac{b^2 + c^2}{c^2 - b^2}\right) - P_{c2}\left(\frac{2c^2}{c^2 - b^2}\right)\right] + (P_{c1} + P_i + P_c)(\boldsymbol{\nu} + \boldsymbol{\nu^2})\right] \tag{29}$$

$$\delta_r = \frac{b}{E_c}\left[(1-\boldsymbol{\nu^2})\left[(P_i+P_c)\left(\frac{b^2+c^2}{c^2-b^2}\right)-P_{c2}\left(\frac{2c^2}{c^2-b^2}\right)\right]+(1-\boldsymbol{\nu^2})(P_{c1})\left(\frac{b^2+c^2}{c^2-b^2}\right)\right.$$
$$\left.+(P_i+P_c)(\boldsymbol{\nu}+\boldsymbol{\nu^2})+(P_{c1})(\boldsymbol{\nu}+\boldsymbol{\nu^2})\right]$$

$$\delta_r = \frac{b}{E_c}\left[(1-\boldsymbol{\nu^2})\left[(P_i+P_c)\left(\frac{b^2+c^2}{c^2-b^2}\right)-P_{c2}\left(\frac{2c^2}{c^2-b^2}\right)\right]\right.$$
$$\left.+(P_{c1})\left((1-\boldsymbol{\nu^2})\left(\frac{b^2+c^2}{c^2-b^2}\right)+(\boldsymbol{\nu}+\boldsymbol{\nu^2})\right)+(P_i+P_c)(\boldsymbol{\nu}+\boldsymbol{\nu^2})\right]$$

$$\delta_r = \frac{b}{E_c}\left[(1-\boldsymbol{\nu^2})\left[(P_i+P_c)\left(\frac{b^2+c^2}{c^2-b^2}\right)-P_{c2}\left(\frac{2c^2}{c^2-b^2}\right)\right]+(P_i+P_c)(\boldsymbol{\nu}+\boldsymbol{\nu^2})\right.$$
$$\left.+(P_{c1})\left((1-\boldsymbol{\nu^2})\left(\frac{b^2+c^2}{c^2-b^2}\right)+(\boldsymbol{\nu}+\boldsymbol{\nu^2})\right)\right]$$

Finally, the expression of P_{c1}during buckling written as:

$$P_{c1} = \frac{\frac{E_c}{b}\delta_r' - \left[(1-\boldsymbol{\nu^2})\left[(P_i+P_c)\left(\frac{b^2+c^2}{c^2-b^2}\right)-P_{c2}\left(\frac{2c^2}{c^2-b^2}\right)\right]+(P_i+P_c)(\boldsymbol{\nu}+\boldsymbol{\nu^2})\right]}{\left((1-\boldsymbol{\nu^2})\left(\frac{b^2+c^2}{c^2-b^2}\right)+(\boldsymbol{\nu}+\boldsymbol{\nu^2})\right)} \quad (30)$$

And P_{c1}during testing only is written as:

$$P_{c1} = \frac{\frac{E_c}{b}\delta_r - \left[(1-\boldsymbol{\nu^2})\left[(P_i)\left(\frac{b^2+c^2}{c^2-b^2}\right)-P_{c2}\left(\frac{2c^2}{c^2-b^2}\right)\right]+(P_i)(\boldsymbol{\nu}+\boldsymbol{\nu^2})\right]}{\left((1-\boldsymbol{\nu^2})\left(\frac{b^2+c^2}{c^2-b^2}\right)+(\boldsymbol{\nu}+\boldsymbol{\nu^2})\right)}$$
$$\frac{\frac{E_c}{b}\delta_r' - \left[(1-\boldsymbol{\nu^2})\left[(P_i+P_c)\left(\frac{b^2+c^2}{c^2-b^2}\right)-P_{c2}\left(\frac{2c^2}{c^2-b^2}\right)\right]+(P_i+P_c)(\boldsymbol{\nu}+\boldsymbol{\nu^2})\right]}{\left((1-\boldsymbol{\nu^2})\left(\frac{b^2+c^2}{c^2-b^2}\right)+(\boldsymbol{\nu}+\boldsymbol{\nu^2})\right)} \quad (31)$$
$$-\frac{\frac{E_c}{b}\delta_r - \left[(1-\boldsymbol{\nu^2})\left[(P_i)\left(\frac{b^2+c^2}{c^2-b^2}\right)-P_{c2}\left(\frac{2c^2}{c^2-b^2}\right)\right]+(P_i)(\boldsymbol{\nu}+\boldsymbol{\nu^2})\right]}{\left((1-\boldsymbol{\nu^2})\left(\frac{b^2+c^2}{c^2-b^2}\right)+(\boldsymbol{\nu}+\boldsymbol{\nu^2})\right)} = 0$$

$$(\delta_r'-\delta_r) = (P_c)\frac{b}{E_c}\left[\frac{\left[(1-\boldsymbol{\nu^2})\left[\left(\frac{b^2+c^2}{c^2-b^2}\right)\right]+(\boldsymbol{\nu}+\boldsymbol{\nu^2})\right]}{\left((\boldsymbol{1}+\boldsymbol{\nu})(1-\boldsymbol{\nu})\left(\frac{b^2+c^2}{c^2-b^2}\right)+\boldsymbol{\nu}(\boldsymbol{1}+\boldsymbol{\nu})\right)}\right]$$

$$(\delta_r' - \delta_r) = (P_c)\frac{b}{E_c}\left[\frac{\left[(1-\nu)\left[\left(\frac{b^2+c^2}{c^2-b^2}\right)\right]+\nu\right]}{\left((1-\nu)\left(\frac{b^2+c^2}{c^2-b^2}\right)+\nu\right)}\right]$$

$$(\delta_r' - \delta_r) = (P_c)\frac{b}{E_c}$$

Experimental Simulation Results

Experimental registrations and simulations are used conjointly to confirm the presence of buckling during the liner pressure test. Simulation tools are generally used when designing downhole tubular, buckling impacts go beyond material elasticity deformation.
Downhole fluid and geometric parameters are presented in the table below:

Table 1. Fluid and geometric parameters

TD (m)	CSG (m)	CSG (7"#)	Mud (sg)	SPACER (sg)	SLURRY (sg)	9"5/8 (m)	DP Do (in)
3342	3341	32	1,45	1,7	1,9	2369	5

The buckling check represents the first step in the tubular design procedure. Simulation results of the neutral point position while pressure test, with the approval of rig registrations, validate the assumption of buckling occurrence. Fig. 2 presents neutral point position variations while testing.

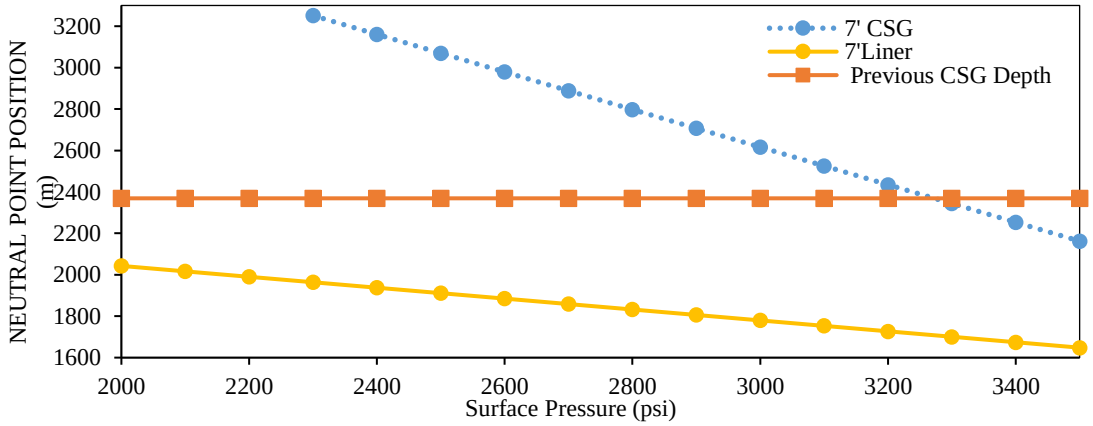

Fig. 2. Casing and liner Neutral point evolution during testing

The red line represents the previous casing depth. Casing column buckling starts in the openhole, and the neutral point (blue line) rises progressively to reach the previous casing at 3200psi. Differently, liner buckling (Yellow line) affects the previous casing section from the beginning.

Examples of buckling during the liner column test are presented in Fig. 3 below:

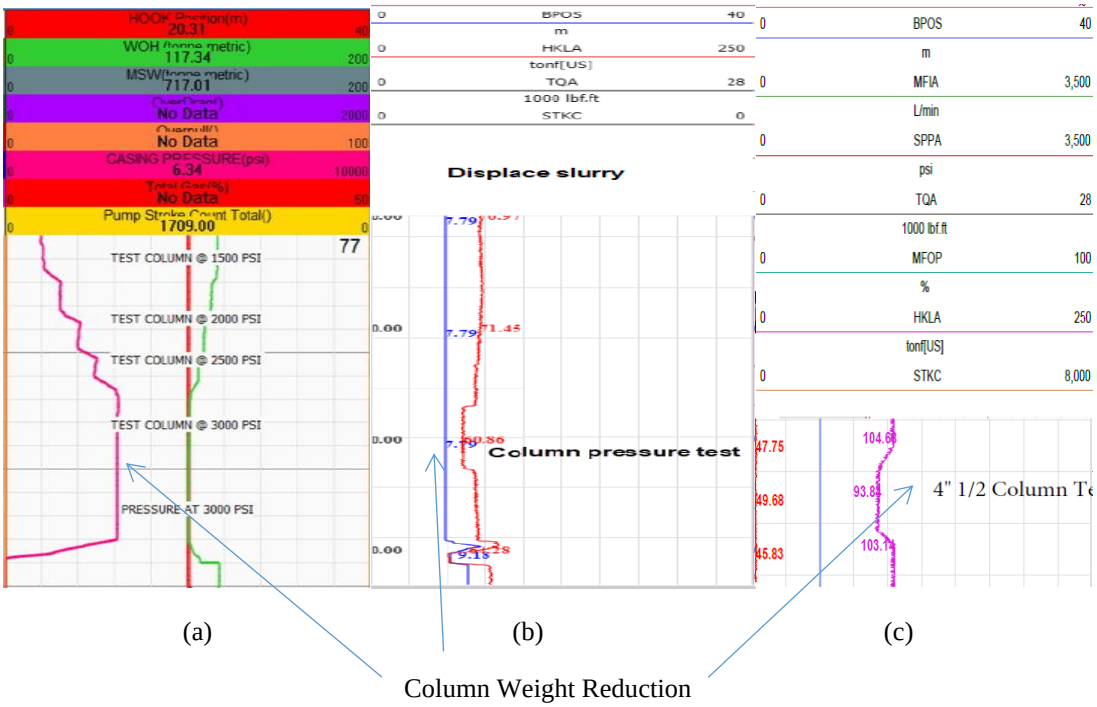

Fig. 3. Buckling registered while liner column test

Reduction in column weight could be easily identified in all column tests presented in Fig. 3. Figs. 3a and 3b represent 7” liner column pressure tests that engender weight reduction of 17T and 11T respectively. In the 4”1/2 liner pressure test, Fig. 3c causes a weight reduction of 11T. Column weight decreases is the image of buckling generation. As pressure rises column receives additional elongation, and accordingly compressive force increases with a remarkable decrease of tension.

In certain situations, the neutral point could move up to the surface (Fig. 4a). While testing, rises of pressure are followed the bay reduction in weight conjointly with the hook budges up. In simulation results presented in Fig.4b, the neutral point reach the surface at around 2400psi. The difference in pressure between simulation and registration is described by the slack-off weight, in real applications neutral point will reach the surface earlier. Fig. 4c points outs that, if a reduction of column weight is registered during testing, bleed-off pressure will engender recovering the initial weight.

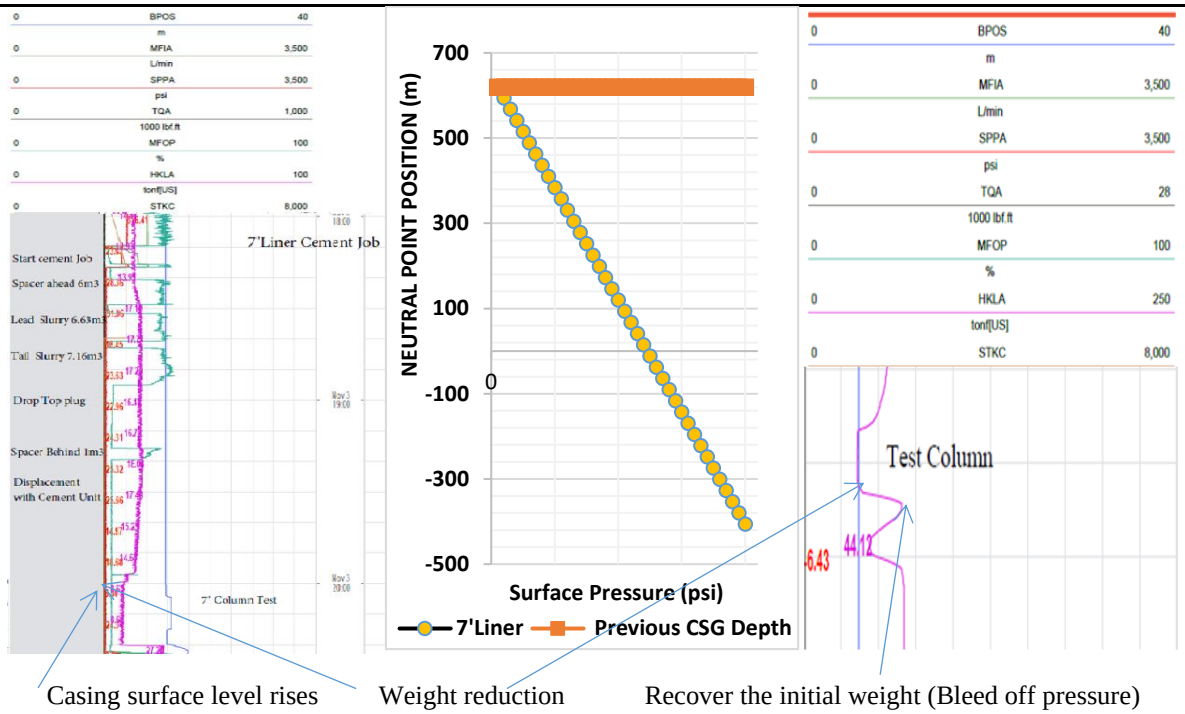

(a) Experimental results (b) Simulation results (c) Test column (Bleed off)

Fig. 4. neutral point moves up to surface

The compression force generated takes an ascending trend, according to the escalation of pressure.

In Fig. 5, rises in pressure produce more additional compressive force in the casing (blue line) compared to the DP running string (yellow line). Therefore, DP remains on the safe side from yield shear stress (red line), compared to the casing where a limit could be achieved at high pressure (gray line).

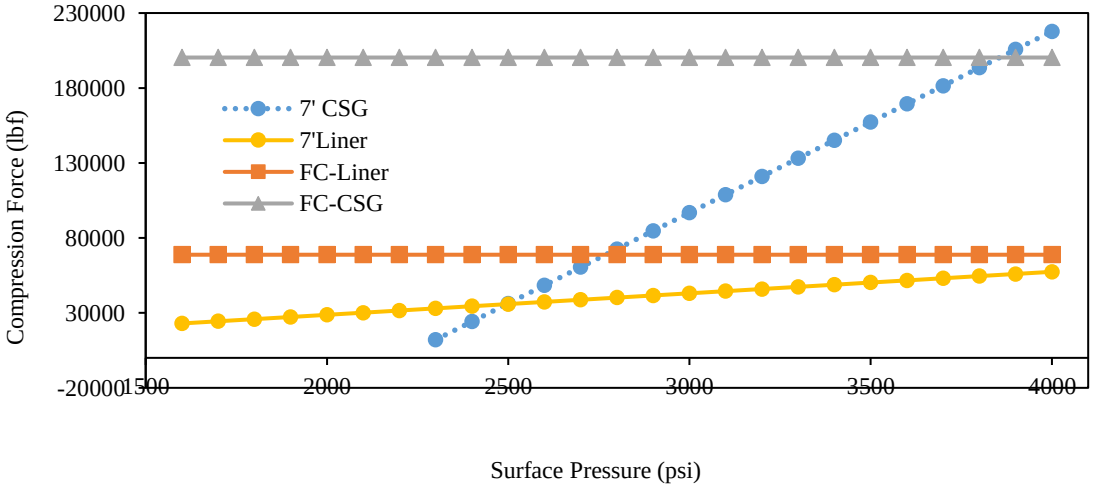

Fig. 5. Casing and liner compressive Force evolution during testing

Fig. 6 gives a comparison of liner and casing contact pressure. It can be seen that the blue and red lines follow the same evolution of pressure.

However, (Fig. 6) liner contact pressure reaches a high level (5600 psi) at 4000 psi testing pressure compared to 2800 psi for casing. In Fig. 7, radial expansion provoked by contact pressure in the liner reaches two times what has been received for the casing. Consequently, stress exerted by contact pressure influences cement sheath behind the casing. Knowing that formation action is constant, effects will be related to compressive strength developed by slurry. In Fig. 8 and Fig. 9, conventional (1.9sg) slurry and lightweight (1.62sg) slurry are investigated

to point out the evolution of stress while rising pressure. In Fig. 8 (1.9sg slurry) radial displacement generated by a liner (0.028in) is around double the one generated by a casing (0.014) at the same pressure test. Inversely, in Fig. 9 (1.62sg slurry) radial displacement developed while testing liner reached 0.164in, compared to 0.018in displacement engendered by casing buckling.

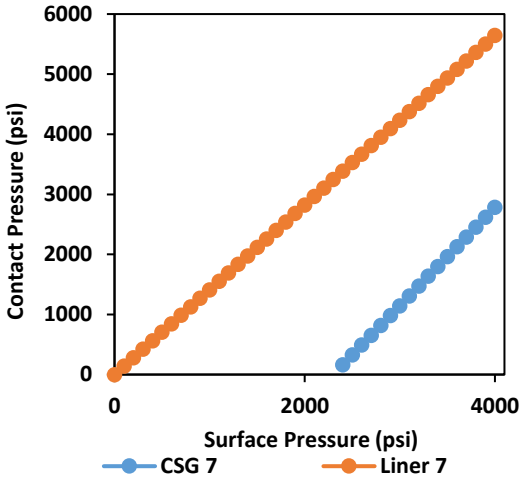

Fig. 6. Contact pressure variation during the test

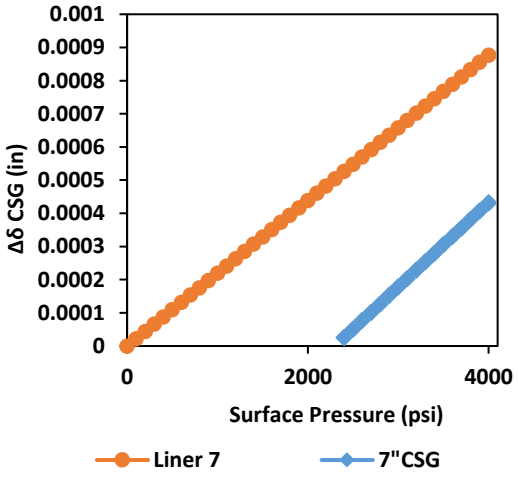

Fig. 7. Radial expansion variation during the test

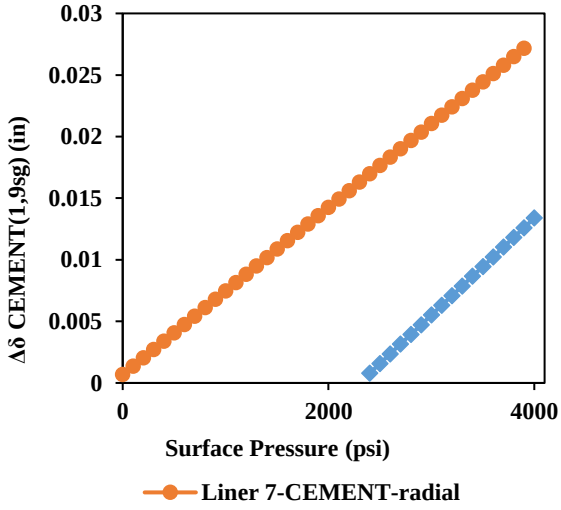

Fig. 8 (1.9 sg) Radial displacement variation during the test

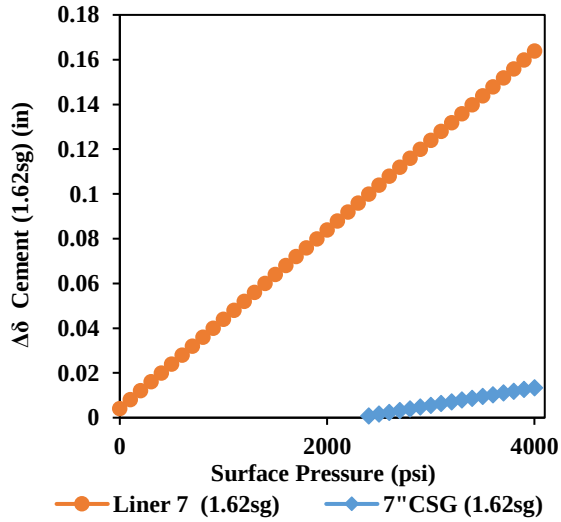

Fig. 9 (1.62) Radial displacement variation during the test

Conjointly with radial displacement and stress, tangential stress will be generated (Fig.10). Tangential stress reaches 2800 psi at 4000 psi liner testing pressure, compared to 1400 psi stress when testing casing at the same pressure range.

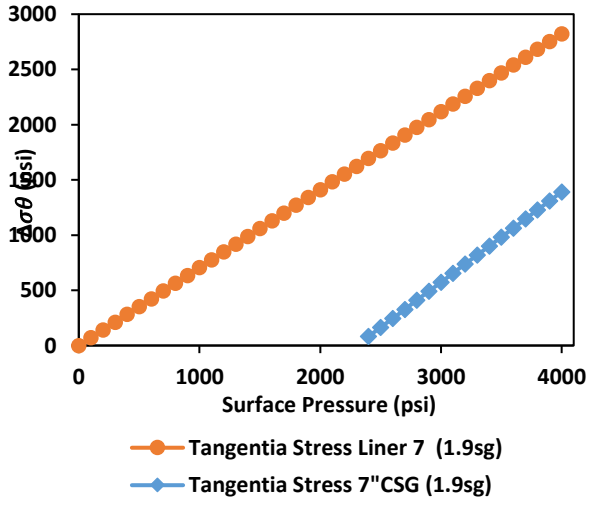

Fig. 10. (1.9 sg) Tangential stress generated while testing liner and casing

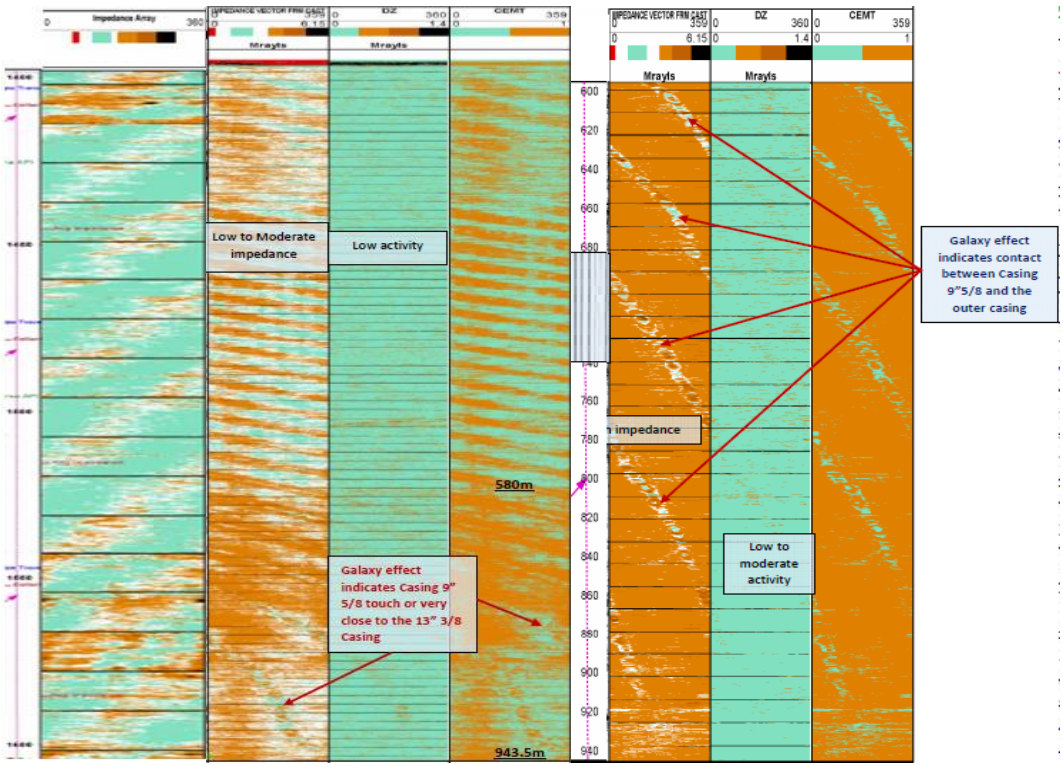

(a) after cement job (b) Before remedial job (c) After remedial job

Fig. 11. Logging has been done after the 9" 5/8 cement job, before and after the remedial job

Fig. 11 points out the presence of helical shape either in open hole Fig. 11a, or overlaps Fig. 11b and 11c. knowing that the remedial job has been done after the 7" liner cement job (at 1200m), pressure testing has been carried out to confirm the integrity of the system. Even though the helical shape appears in the early primary cement log, 7 " liner cementing, and testing could aggravate the situation.

Further studies could be oriented to point out detailed influences of buckling on previous casing Cement sheath, formation, and down-hole equipment conjointly with long liner buckling initiation.

Conclusion

Based on spring theory, tubular helical buckling theory, interface continuity condition theory, and via stress analysis method the influences of buckling while liner testing is elucidated.

Rising contact force acting on previous casing during testing may affect cement behind. Radial displacement for both conventional (1.9sg) and lightweight slurry confirm the influence of cement type on the radial displacement stress. Tangential stress generated while testing liner and casing are investigated, and results confirm that the liner system produces more stress compared to the casing.

Buckling is confirmed through rig registrations and simulations, passing by neutral point position and contact force exerted to approve the gravity of the situation. Finally, the helical shape recorded by logging may become worst and affect the integrity of cement.

Nomenclature

F_b:	Buckling force, (lb_f)
A_i:	Area of DP internal diameter (in^2)
P_i:	Equivalent inside bottom pressure (psi)
E:	String elongation (in)
W_s:	Weight of steel per unit length (lb_f /in)
W_o:	Weight of fluid outside casing per unit length (lb_f /in)
F_{bN}:	New buckling force (lb_f)
F_b :	Buckling force (lb_f)
F_N :	contact force (lb_f)
E, :	Young modulus and poisons ratio of the tubular
R_e;E_e :	Equivalent radius and Young modulus respectively
$\sigma_{R:in-CSG}$:	Inside casing stress
d :	DP diameter (in)
t :	Half of the tensile yield (psi)
σ_z , δ_r , σ_θ :	Axial, Radial, and Circumferential stress
r_m:	Mean radius of the casing
Pi	Internal pressure
Pc1:	Contact pressure at cement–casing interface
a:	Internal casing radius
c:	Outer cement sheath radius
F_a:	DP tension force. (lb_f)
A_o:	Area of DP outer diameter (in^2)
P_o:	Equivalent annulus bottom pressure (psi)
W :	Buoyed weight per unit length (lb_f /in)
W_i:	Weight of fluid inside casing (lb_f /in)
F_{cr} :	Compressive force (lb_f)
P_{Pitch} :	Helix pitch (in)
R_1, R_2 :	Radius of DP and casing respectively
P_{max} :	Maximum surface pressure reached
$\sigma_{R:out-Cem}$:	Stress exerted on cement
D:	Previous casing inside diameter (in)
ε_θ, ε_z :	Hoop and axial strain
σ'_r, σ'_θ:	Buckling Radial, Circumferential stress
t_s	Thickness of the casing
Pc:	Contact pressure engenders by buckling
P_{test}:	Surface pressure test
b:	Internal cement sheath radius
F_{critic}:	The critical force required to raise maximum shear to reach minimum yield shear of DP (lbs)

References

[1] Richard J. Davies a, Sam Almond a, Robert S. Ward b, Robert B. Jackson c,d, Charlotte Adams a, Fred Worrall a, Liam G. Herringshawa, Jon G. Gluyas a, Mark A. Whiteheade (2014)" Oil and gas wells and their integrity: Implications for shale and unconventional resource exploitation" Marine and Petroleum Geology. http://dx.doi.org/10.1016/j.marpetgeo.2014.03.001

[2] Kiran, R., Teodoriu, C., Dadmohammadi, Y., Nygaard, R., Wood, D., Mokhtari, M., Salehi, S., (2017) "identification and evaluation of well integrity and causes of failure of well integrity barriers (A review) " Journal of Natural Gas Science & Engineering. https://doi.org/10.1016/j.jngse.2017.05.009

[3] Mohammed, A.I., Oyeneyin, B., Atchison, B. And Njuguna, J. (2019) "Casing structural integrity and failure modes in a range of well types: a review" Journal of natural gas science and engineering, 68, article ID 102898. https://doi.org/10.1016/j.jngse.2019.05.011

[4] API Recommended practice for drill stem design and operating limits. 7G 16th Edition, August 1998.

[5] William C., Gary J. P., Michael D. L. (2016) "Standard Handbook of Petroleum and Natural Gas Engineering". Third Edition. 2016, (Chapter 4), Drilling and Well Completions. Elsevier. Pages 4-1-4-584.

[6] Hebert, R.N., 1986. Liner cementing techniques and case histories offshore Western Gulf of Mexico. SPE-14777-MS. In: Presented at the IADC/SPE Drilling Conference, 10-12 February, Dallas, Texas. https://doi-org.ezproxy.lib.ou.edu/10.2118/14777-

[7] Klinkenberg A (1951) "The neutral zones in drill pipe and casing and their significance in relation to buckling and collapse" drilling and production practice. American Petroleum Institute, pp. 64–76.

[8] Yinping Cao, Hui Xia, and Yihua Dou (2017) "Strength analysis of helical buckling tubing using spring theory" AIP Conference Proceedings 1864, 020163; https://doi.org/10.1063/1.4992980

[9] Lubinski, A., W.S. Althouse, and J.L. Logan, (1962) "Helical Buckling of Tubing Sealed in Packers" SPE Journal of Petroleum Technology, Vol. 14, N°6, pp. 655-670. https://doi.org/10.2118/178-PA

[10] Chen, Y. C.; Lin, Y. H and Cheatham, J. B. (1990) "Tubing and casing Buckling in Horizontal wells" J PET Technology Vol.42 N° 2. Pp. 140-191. SPE-1976-PA. https://doi.org/10.2118/19176-PA

[11] Mitchell, R.F. (1999) "Buckling Analysis in Deviated Wells: A Practical Method" SPE Drill & Compl 14 (1): 11-20. SPE-55039-PA. https://doi.org/10.2118/55039-PA

[12] Mitchell, R.F. (1986) ‘‘Simple Frictional Analysis of Helical Buckling of Tubing,’’ SPE Drill Eng. Vol.1 N°06. Pp. 457–465. https://doi.org/10.2118/13064-PA

[13] De-Li Gao, Wen-Jun Huang (2015) "A review of down-hole tubular string buckling in well engineering" Pet. Sci. 12:443–457. DOI 10.1007/s12182-015-0031-z

[14] Gao DL, Liu FW, Xu BY. (1998) "An analysis of helical buckling of long tubulars in horizontal wells" SPE

[15] Dawson, R. and Paslay, P.R. (1985) “Drillpipe Buckling in Inclined Holes”. J Pet Technol 36 (10): 1734–1738. https://doi.org/10.2118/11167-PA

[16] Barakat ER, Miska SZ, Yu M, et al. (2007) "The effect of hydraulic vibrationson initiation of buckling and axial force transfer for helically buckled pipes at simulated horizontal wellbore conditions. SPE/IADC drilling conference, 20–22 February. http://dx.doi.org/10.2118/105123-MS.

[17] Daily JS, Ring L, Hajianmaleki M, et al. (2013) "Critical buckling load assessment of drill strings in different wellbores using the explicit finite element method" SPE offshore europe oil and gas conference and exhibition, Aberdeen, http://dx.doi.org/10.2118/166592-MS.

[18] Dellinger T, Gravley W, Walraven JE. Preventing buckling in drill string. US patent: (1983), 4384483.

[19] Gao GH, Miska SZ. (2009) "Effects of boundary conditions and friction on static buckling of pipe in a horizontal well. SPE J.;14(4):782–796. https://doi.org/10.2118/111511-PA

[20] Gao GH, Miska SZ. (2010a) "Effects of friction on post–buckling behavior and axial load transfer in a horizontal well. SPE J.;15(4):1104–1118. https://doi.org/10.2118/120084-PA

[21] Jellison M.J., Brock J.N. (2000) "The Impact of Compression Forces on Casing-String Designs and Connectors" SPE Drill. & Completion N° 15, Vol. 4, pp 241-248. https://doi.org/10.2118/47790-MS

[22] Yinping Cao, Hui Xia and Yihua Dou (2017) " Strength analysis of helical buckling tubing using spring theory" Green Energy and Sustainable Development I, AIP Conf. Proc. 1864, 020163-1–020163-7; https://doi.org/10.1063/1.4992980

[23] M J Fagan1¤ and J McConnachie2 "A review and detailed examination of non-layered conformal contact by finite element analysis" JOURNAL OF STRAIN ANALYSIS VOL 36 NO 2; pp.177-195

[24] Arnfinn N., Naval A. (2017) "The Magic of Buoyancy and Hydrostatics –Buoyancy and Effective Forces" Modern Applied Science; Vol. 11, No. 12, pp 77-83. DOI:10.5539/mas. v11n12p77

[25] Eirik Kaarstad '2011) " Theory and Application of Buoyancy in Wells" Modern Applied Science Vol. 5, No. 3, June. https://doi.org/10.2118/101795-MS

[26] Arnfinn Nergaard (2017) "The Magic of Buoyancy and Hydrostatics –Buoyancy and Effective Forces" Modern Applied Science; Vol. 11, No. 12; pp.77-83;

[27] Clark H. C. (1987) "Mechanical Design Considerations for Fracture-Treating Down Casing Strings" SPE Drilling Engineering. June 1987 pp.116-126. DOI:10.2118/14370-PA

[28] De Andrade J. Sangesland S. Skorpa R. Todorovic J.; Vralstad T. (2016) "Experimental laboratory setup for visualization and quantification of cement-sheath integrity". SPE Drilling & Completion; Vol.31 N°04. pp. 317 – 326. https://doi.org/10.2118/173871-PA

[29] Catalin T., Christian K., Mahmood A., Jerome S., Arash S., (2013) "wellbore integrity and cement failure at hpht conditions". International Journal of Engineering and Applied Sciences. Vol. 2, No.2

[30] S. Pelipenko and I.A. Frigaard (2004) "Mud removal and cement placement during primary cementing of an oil well" Part 2; steady-state displacements; Journal of Engineering Mathematics 48: 1–26, https://doi.org/10.1023/B:ENGI.0000009499.63859.f0

[31] Kevin N. L., Mtaki T. M., Qinggui W., Haiyang H., Jun G. (2019) "Experimental study on oil based mudcake removal and enhancement of shear bond strength at cement-formation interface" Journal of Petroleum Science and Engineering. Vol. 176, pp. 754-761. https://doi.org/10.1016/j.petrol.2019.01.066

[32] Jiwei J., Jun L., Gonghui L., Yan X. and Wai L. (2019) "Influence of Casing Pressure Test on Seal Integrity of Cementing First Interface" Trans Tech Publications Ltd, Switzerland. Vol. 944, pp 1020-1027. DOI: 10.4028/www.scientific.net/MSF.944.1020

[33] Xuelin Donga, Zhiyin Duanb, Zhe Quc, Deli Gaoa (2019) " Failure analysis for the cement with radial cracking in HPHT wells based on stress intensity factors" Journal of Petroleum Science and Engineering N 179, pp. 558–564.

[34] Leksir A. (2020) "Maximum allowable pressure during heavy slurry displacement" Journal of Petroleum Exploration and Production Technology Vol.10 N°7 pp: 2829–2844. DOI: 10.1007/s13202-020-00959-5

[35] Wahl, A.M., 1963: "Mechanical Springs," 2nd Ed., McGraw-Hill Book Company, New York.

[36] Teodoriu, Catalin, Ugwu, Ignatius, and Jerome Schubert. (2010) "Estimation of Casing-Cement-Formation Interaction using a new Analytical Model." Paper presented at the SPE EUROPEC/EAGE Annual Conference and Exhibition, Barcelona, Spain, June 2010. doi: https://doi.org/10.2118/131335-MS

How to cite: Abdeslem L. Liner Pressure Test Buckling Generation and Influences on Running String and Cement Quality of Previous Casing in Vertical Wells. Journal of Chemical and Petroleum Engineering. 2023; 57(1): 149-165.